Electron energy-loss spectrum of nanowires

G. F. Bertsch
Institute of Nuclear Theory and Department of Physics, University of Washington, Box 351560, Seattle, Washington 98195

H. Esbensen
Physics Division, Argonne National Laboratory, Argonne, Illinois 60439

B. W. Reed
School of Applied and Engineering Physics, Cornell University, Ithaca, New York 14853
(Received 8 May 1998)

The electronic properties of nanoscale-size fibers can be studied by electron energy-loss spectroscopy with electron beams that pass near the fiber but do not penetrate it. We derive the formulas for the differential energy spectrum assuming that the fiber can be treated as a dielectric cylinder. The formula can be evaluated in closed form for a conducting wire; the spectrum displays the surface plasmon and a low-energy peak associated with charge-conduction modes that diverges inversely as the energy loss. [S0163-1829(98)05239-4]

I. INTRODUCTION

The study of needles and wires on the nanometer scale has been an active and growing area of research. An important problem is to characterize their electronic properties. In principle, information about their electron response can be obtained from electron energy-loss spectroscopy (EELS), using the same electron microscope optics as is used to image the needles. An experimental study of the plasmons in carbon nanotubes was reported in Ref. 1. The present article is motivated by an experimental study of the low-energy excitations of small silicon whiskers.[2] More commonly, the high-energy loss spectrum associated with core excitation is used to probe the chemical composition of the structures.[3] A review of EELS applied to small particles and interfaces is given by Ref. 4. In this work we present a general formalism for calculating the electron energy-loss spectrum for electrons passing close to a dielectric cylinder or tube without penetrating it. We consider only the geometry where the electron beam is perpendicular to the needle, and the main result is derived in the next section, Eq. (19) below. The case where the electron beam is parallel to the axis of a cylinder has been given in Ref. 5. A general formula for solid cylinders only is given in Ref. 6. The perpendicular geometry has also been considered with the neglect of the modes parallel to the axis in Ref. 7.

A general formulation of the interaction of dielectric cylinders with the electromagnetic field is given in Ref. 8, expanding the fields in cylindrical functions. The interaction with external charges is treated in a similar way, using classical electromagnetism and an expansion in cylindrical functions. The energy spectrum is then calculated classically, as in the derivation of the formula for the plasmon excitation of electrons passing through thin foils.[9] The energy-loss spectrum is intrinsically quantum mechanical, but in the derivation the quantum mechanics only enters by identifying the energy loss with a frequency.

The derivation assumes that the electron travels on a straight line with uniform velocity and passes by the fiber without penetrating it. This allows an analytic integration of the integral for the energy loss along the path of the electron, leaving only an integral over the wave vector of the excitation along the axis of the fiber. Penetrating electrons can be treated the same way, but then all the integrals must be done numerically, and the interaction is more complicated because of the screening of the electron and the excitation of the bulk plasmon. We will also make a nonrelativistic approximation on the electromagnetic field, assuming it to be the same as the electric field of the electron in its rest frame.

As an application of the formula, we compute the energy-loss spectrum for a conducting wire. In this case the integral over wave numbers can be done analytically to give a closed form expression. The energy-loss spectrum exhibits two peaks: the ordinary surface plasmon and a diverging peak toward zero energy associated with charge conduction along the axis of the wire.

II. EELS FOR NONPENETRATING ELECTRONS

We begin with some definitions. We consider a cylinder of radius R located on the z axis of the coordinate system. The trajectory of the electron is given by $\vec{r}_e(t)=(b,vt,0)$ where b is the impact parameter on the cylinder axis and v is the velocity of the electron. We will use cylindrical coordinates (ρ,ϕ,z). The presence of the electron induces a charge density $\sigma_s\delta(\rho-R)$ on the surface of the cylinder, which in turn produces an induced Coulomb potential Φ_s and a force on the electron $e\vec{\nabla}\Phi_s$, where e is the magnitude of the electron's charge.

The energy loss of the electron is given by the integral

$$\Delta E=-e\int_{-\infty}^{\infty}dt\vec{v}\cdot\vec{\nabla}\Phi_s(\vec{r}_e,t)=-e\int_{-\infty}^{\infty}dtv\,\frac{\partial\Phi_s(\vec{r}_e,t)}{\partial y}. \tag{1}$$

To obtain the energy-loss spectrum from this integral, we must use the Fourier representation of the time-dependent induced potential,

$$\Phi_s(\vec{r},t)=\int_{-\infty}^{\infty}\frac{d\omega}{2\pi}\exp(-i\omega t)\tilde{\Phi}_s(\vec{r},\omega).$$

Inserting this into Eq. (1) together with the trajectory $y=vt$ the energy loss becomes

$$\Delta E=-e\int_{-\infty}^{\infty}dy\int\frac{d\omega}{2\pi}\exp(-i\omega y/v)\frac{\partial\tilde{\Phi}_s(\vec{r},\omega)}{\partial y}. \quad (2)$$

Next we make a partial integration over y, and combine the positive and negative frequency domains into a single integration over positive frequencies. This yields

$$\Delta E=\int_{-\infty}^{\infty}d\omega\omega g(\omega)=\int_0^{\infty}d\omega\omega[g(\omega)-g(-\omega)], \quad (3)$$

where

$$g(\omega)=-\frac{ie}{2\pi v}\int_{-\infty}^{\infty}dy\ \exp(-i\omega y/v)\tilde{\Phi}_s(\vec{r},\omega). \quad (3')$$

In Eq. (3) we changed the integration limits to positive frequencies. Converting the frequencies to energies with $E=\hbar\omega$, the coefficient of $\hbar\omega$ in the integrand may be interpreted as the energy-loss probability distribution dP/dE. It is given by

$$\frac{dP}{dE}=\frac{2}{\hbar^2}\,\mathrm{Re}\ g(\omega)=\frac{e}{\hbar^2\pi v}\,\mathrm{Im}\int_{-\infty}^{\infty}dy \times\exp(-i\omega y/v)\tilde{\Phi}_s(\vec{r},\omega), \quad (4)$$

where we have used $g(\omega)-g(-\omega)=2\,\mathrm{Re}\,g(\omega)$, which follows from causality. We will apply Eq. (4) by relating the induced potential Φ_s to the induced charge and the potential from the electron.

When an external field polarizes a dielectric, the polarization charge resides on the surface of the dielectric, irrespective of its shape. The surface charge density $\sigma_s(\phi,z)$ gives rise to the induced potential. Two relations are required to determine them in terms of the external field Φ_{ext}. The first is Gauss's theorem relating the normal components of the electric field inside and outside the dielectric. Denoting the normal components of the electric field just outside and just inside the cylinder by E_+ and E_-, respectively, we require $4\pi\sigma_s=E_+-E_-$. The second relation is the dielectric formula $\tilde{E}_+=\epsilon\tilde{E}_-$, where ϵ is the frequency-dependent dielectric function and the tildes denote functions that have been Fourier transformed in time. Combining these equations gives

$$4\pi\tilde{\sigma}_s=\frac{\epsilon(\omega)-1}{\epsilon(\omega)}\tilde{E}_+. \quad (5)$$

The normal electric field $\tilde{E}_+$ is related to the potentials by

$$\tilde{E}_+=-\frac{\partial}{\partial\rho}(\tilde{\Phi}_s+\tilde{\Phi}_{\mathrm{ext}}). \quad (5')$$

To calculate the potentials Φ_s and Φ_{ext} we shall make use of the Green function which is a solution to

$$\nabla^2G(\vec{r},\vec{r}')=-4\pi\delta(\vec{r}-\vec{r}').$$

Expressed in terms of the cylindrical coordinates (ρ,ϕ,z) it has the form[10]

$$G(\vec{r},\vec{r}')=4\pi\sum_m\frac{e^{im(\phi-\phi')}}{2\pi} \times\int_{-\infty}^{\infty}\frac{dk}{2\pi}e^{ik(z-z')}I_m(|k|\rho_<)K_m(|k|\rho_>), \quad (6)$$

where I_m and K_m are the usual Bessel functions of imaginary argument. We represent the surface charge density in a cylindrical expansion,

$$\sigma_{mk}^s=\int_0^{2\pi}d\phi\int_{-\infty}^{\infty}dz e^{-im\phi}e^{-ikz}\sigma_s(\phi,z) \quad (7)$$

and similarly for the potentials. We then obtain the following equation for the induced potential outside the cylinder

$$\Phi_s=\int\int\int\rho'd\rho'd\phi'dz'G(\vec{r},\vec{r}')\sigma_s(\phi',z')\delta(\rho'-R) =\frac{1}{\pi}\sum_m e^{im\phi}\int dke^{ikz}RI_m(|k|R)K_m(|k|\rho)\sigma_{mk}^s, \quad (8)$$

which may also be represented as

$$\Phi_s(\rho,\phi,z)=\frac{1}{4\pi^2}\sum_m e^{im\phi}\int_{-\infty}^{\infty}dke^{ikz}\Phi_{mk}^s(\rho),$$

with

$$\Phi_{mk}^s(\rho)=4\pi RI_m(|k|R)K_m(|k|\rho)\sigma_{mk}^s. \quad (9)$$

Obviously, the same relation holds between the Fourier transformed quantities $\tilde{\sigma}_{mk}^s$ and $\tilde{\Phi}_{mk}^s$. We now combine this with Eq. (5) to eliminate the induced field. Equation (5) in the cylindrical representation is

$$4\pi\tilde{\sigma}_{mk}^s=-(1-1/\epsilon)\frac{\partial}{\partial\rho}(\tilde{\Phi}_{mk}^s+\tilde{\Phi}_{mk}^{\mathrm{ext}})_{\rho=R}=-(1-1/\epsilon) \times\left(4\pi kRI_m(|k|R)K_m'(|k|\rho)\tilde{\sigma}_{mk}^s+\frac{\partial}{\partial\rho}\tilde{\Phi}_{mk}^{\mathrm{ext}}\Big|_{\rho=R}\right).$$

Solving for the surface charge, we obtain

$$4\pi\tilde{\sigma}_{mk}^s=\Pi_{mk}\frac{d\tilde{\Phi}_{mk}^{\mathrm{ext}}}{d\rho}\Big|_{\rho=R}, \quad (10)$$

where

$$\Pi_{mk}=\frac{(1-\epsilon)}{\epsilon+(\epsilon-1)xI_m(x)K_m'(x)},\quad x=|k|R \quad (11)$$

represents the frequency-dependent response of the wire. Using the Wronskian identity $xI_m'(x)K_m(x)-xI_m(x)K_m'(x)=1$, this can also be written as

$$\Pi_{mk}=\frac{(1-\epsilon)}{1+(\epsilon-1)xI_m'(x)K_m(x)}. \quad (11')$$

A. External field

The external field from the moving electron is

$$\Phi_{\rm ext}(\vec{r},t)=\frac{-e}{|\vec{r}-\vec{b}-\vec{v}t|}=\frac{-4\pi e}{(2\pi)^3}\int d^3k \times\frac{\exp[ik_x(x-b)+ik_y(y-vt)+ik_z z]}{k^2}.$$

We are interested in the Fourier transform with respect to time,

$$\tilde{\Phi}_{\rm ext}(\vec{r},\omega)=\frac{-4\pi e}{v(2\pi)^2}e^{i\omega y/v}\int\int dk_x dk_z \times\frac{\exp[ik_x(x-b)+ik_z z]}{k_x^2+k_z^2+(\omega/v)^2}. \quad (12)$$

This integral can be performed in closed form to obtain

$$\tilde{\Phi}_{\rm ext}(\vec{r},\omega)=\frac{-2e}{v}e^{i\omega y/v}K_0\left(\frac{\omega}{v}\sqrt{z^2+(x-b)^2}\right) \quad (13)$$

but this is not convenient for the cylindrical geometry of the present problem. To transform to the (m,k,ρ) representation we note that k may be identified with k_z in Eq. (12), and the remaining k_x integration can be done analytically to obtain

$$\tilde{\Phi}^{\rm ext}_{mk}(\rho,\omega)=\frac{-2\pi e}{v}\int_0^{2\pi}d\phi e^{-im\phi}e^{i\omega y/v} \times\frac{\exp[-|b-x|\sqrt{k^2+(\omega/v)^2}]}{\sqrt{k^2+(\omega/v)^2}}, \quad (14)$$

where $x=\rho\cos\phi$ and $y=\rho\sin\phi$. Remembering that $\rho<b$ for an external electron, we can rewrite Eq. (14) as

$$\Phi^{\rm ext}_{mk}(\rho,\omega)=\frac{-(2\pi)^2 e}{v}\frac{\exp[-b\sqrt{k^2+(\omega/v)^2}]}{\sqrt{k^2+(\omega/v)^2}}C_{mk}(\rho,\omega), \quad (15)$$

where

$$C_{mk}(\rho,\omega)=\int_0^{2\pi}\frac{d\phi}{2\pi}e^{-im\phi}e^{i\omega\rho\sin(\phi)/v} \times\exp[\cos(\phi)\rho\sqrt{k^2+(\omega/v)^2}]. \quad (15')$$

The integral Eq. (15′) can be expressed in terms of the I_m Bessel function[11] as

$$C_{mk}=\left(\frac{\sqrt{k^2+(\omega/v)^2}+\omega/v}{|k|}\right)^m I_m(|k|\rho). \quad (15'')$$

Another expression for Φ_{mk} may be derived from the Green function, Eq. (6). This gives directly the field of the electron as

$$\Phi^{\rm ext}_{mk}(\rho,t)=-4\pi e\left(\frac{b-ivt}{\sqrt{b^2+(vt)^2}}\right)^m \times I_m(|k|\rho)K_m[|k|\sqrt{b^2+(vt)^2}].$$

The required Fourier transform in time is

$$\tilde{\Phi}^{\rm ext}_{mk}(\rho,\omega)=\frac{-4\pi eb}{v}I_m(|k|\rho)F_m(\xi,kb), \quad (16)$$

where

$$F_m(\xi,u)=\int_{-\infty}^{\infty}dw e^{i\xi w}\left(\frac{1-iw}{\sqrt{1+w^2}}\right)^m K_m(|u|\sqrt{1+w^2}) \quad (17)$$

and

$$\xi=b\omega/v.$$

The parameter ξ is the well-known adiabaticity parameter in the theory of Coulomb excitation. Comparing Eqs. (16) and (17) with our previous expression for $\Phi^{\rm ext}_{mk}$, Eqs. (15)–(15″), we see that the integral F_m is analytic and given by

$$F_m(\xi,u)=\frac{\pi e^{-\sqrt{u^2+\xi^2}}}{\sqrt{u^2+\xi^2}}\left(\frac{\sqrt{u^2+\xi^2}+\xi}{|u|}\right)^m. \quad (17')$$

B. Collecting all terms

Let us now collect all terms that are needed to calculate the energy-loss spectrum from Eq. (4). We first go from the external potential to the induced charge by Eqs. (10), (11), and (17). These combine to give

$$\tilde{\sigma}^s_{mk}=-\Pi_{mk}\frac{keb}{v}I'_m(x)F_m(\xi,kb).$$

This is inserted into Eq. (9) for the induced potential. We need the induced potential Eq. (8) evaluated at the electron position $(b,y,0)$. This is

$$\tilde{\Phi}_s=-\frac{1}{\pi}\sum_m\int_{-\infty}^{\infty}dk\left(\frac{b+iy}{\rho}\right)^m \times RI_m(x)K_m(|k|\rho)\Pi_{mk}\frac{|k|eb}{v}I'_m(x)F_m(\xi,kb),$$

where $\rho=\sqrt{b^2+y^2}$. Inserting the induced potential in Eq. (4) we obtain

$$\frac{dP}{dE}=\frac{e^2b}{\pi^2\hbar^2v^2}\sum_m\int_{-\infty}^{\infty}dk|k|RI_m(x)I'_m(x) \times{\rm Im}\,\Pi_{mk}F_m(\xi,kb)\int_{-\infty}^{\infty}dy e^{-i\omega y/v}\left(\frac{b+iy}{\rho}\right)^m \times K_m(|k|\rho). \quad (18)$$

The integral over y is just the complex conjugate of $bF_m(\xi,kb)$ defined in Eqs. (16) and (17). We thus obtain as our final expression for the energy-loss probability distribution

$$\frac{dP}{dE}=\frac{e^2b^2}{\pi^2\hbar^2v^2}\sum_m\int_{-\infty}^{\infty}dkxI_m(x)I'_m(x) \times{\rm Im}\,\Pi_{mk}|F_m(\xi,kb)|^2,\quad x=|k|R. \quad (19)$$

Notice that the quantities on the left hand side are real except for the needle response Π, so the required imaginary part in Eq. (4) comes entirely from Im Π.

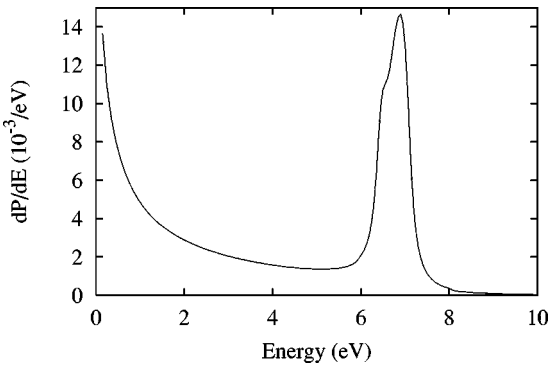

FIG. 1. Electron energy-loss spectrum of a conducting wire for representative conditions: $b=35$ Å, $R=35$ Å, and the electron energy is 100 keV. The dielectric function is given by Eq. (20) with $\omega_p=10$ eV and $\hbar/\tau=0.25$ eV.

Equation (19) is just the structure that would be obtained from a quantum mechanical derivation. Quantum mechanically the probability would be calculated using time-dependent perturbation theory, which gives the rate as an amplitude squared times a density of final states. The $|F|^2$ provides the squared amplitude, and the Im Π is the density of wire excitations weighted by the squares of their transition strengths.

Our derivation is nonrelativistic in that the electric field was taken to be the same as the field in the rest frame of the electron. The electron kinematics is already relativistic if the velocity is computed correctly. The Lorentz contraction of the electric field affects only the adiabaticity parameter ξ, which is decreased by a factor $\sqrt{1-(v/c)^2}$ as a result. Other relativistic effects associated with magnetic fields are not included in our treatment; to incorporate these the theory would have to be generalized to magnetic excitations.

III. WIRE RESPONSE

In this section we apply the theory to the response of a conducting wire. The dielectric function of a Drude conductor is given by

$$\epsilon(\omega)=1-\frac{4\pi ne^2}{m\omega(\omega+i/\tau)}, \tag{20}$$

where n is the electron density. The bulk plasmon frequency ω_p may be found from the zero of $\epsilon(\omega)$, thus $\omega_p^2=4\pi e^2 n/m$. Similarly, the resonant modes in the wire can be determined by requiring that the denominator vanish in Eq. (11′),

$$1+(\epsilon-1)xI_m'(x)K_m(x)=0.$$

This may be solved for the frequency ω_{mk} of the mk mode,

$$\omega_{mk}^2=\omega_p^2 xI_m'(x)K_m(x). \tag{21}$$

This expression was derived in Ref. 12 as the frequency shift of optical phonons in a cylindrical dielectric. This formula has simple limits when kR is small. For $m=0$, the Bessel functions of small argument are $I_0'(x)\approx x/2$ and $K_0(x)\approx-\ln(x)$. This gives the resonance condition

$$\omega_{0k}^2=\omega_p^2\frac{(kR)^2}{2}\ln\left(\frac{1}{kR}\right).$$

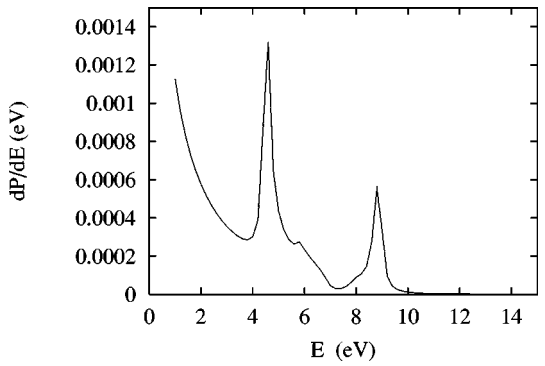

FIG. 2. Electron energy-loss spectrum of a hollow conducting tube having the same dielectric function as in Fig. 1, for 100 keV electrons at an impact parameter of $b=10$ Å. The geometric parameters of the tube are $R_1=5$ Å and $R_2=8.5$ Å, corresponding to the (10,10) monolayer graphitic carbo nanotube.

This dispersion of wire modes has been derived in Refs. 13 and 14. We see that the frequency goes to zero as the wavelength gets large. For $m\neq0$, the approximate Bessel functions are $I_m(x)\approx(x/2)^m/m!$ and $K_m(x)\approx(m-1)!(2/x)^m/2$. Equation (21) then yields the frequency

$$\omega_{mk}^2=\frac{1}{2}\omega_p^2, \quad m\neq0.$$

This is exactly the surface plasmon formula, showing that the long-wavelength azimuthal modes have the same frequency as the modes on a planar surface.

To compute an energy-loss spectrum for the wire, we need the imaginary part of the response which can be expressed as

$$\text{Im }\Pi=-\frac{\pi}{Rd[xI_m'(x)K_m(x)]/dx}\,\delta(k-k_{m\omega}),$$

where $k_{m\omega}$ is the value of k that satisfies Eq. (21) for given ω, and $x=k_{m\omega}R$ here. Inserting this in Eq. (19), the k integration can be carried out to give an entirely analytic expression for the energy-loss probability distribution,

$$\frac{dP}{dE}=\frac{e^2b^2}{\pi\hbar^2v^2R}\sum_m\frac{xI_m(x)I_m'(x)}{d[xI_m'(x)K_m(x)]/dx}|F_m(\xi,k_{m\omega}b)|^2. \tag{22}$$

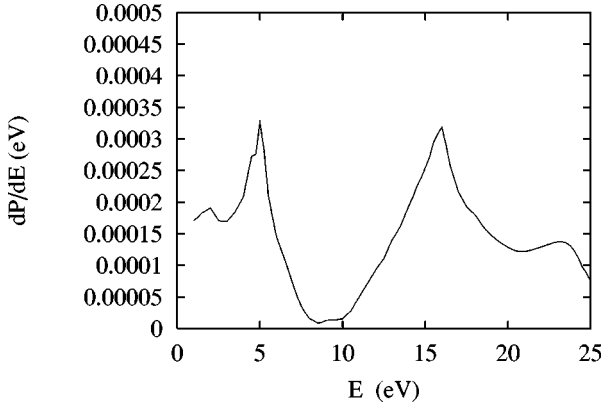

FIG. 3. Electron energy-loss spectrum of a (10,10) graphite nanotube, taking the empirical dielectric function of graphite (Ref. 17). The other parameters are the same as in Fig. 2.

For $m \neq 0$, the modes will be the surface plasmons located near $\omega = \omega_p/\sqrt{2}$. The behavior at small energy loss is more complicated. Only the $m=0$ mode allows a solution for $k_{m\omega}$ when ω is small. The ratio in Eq. (22) varies as $k_{0\omega}/\ln(k_{0\omega})$ in this limit. However, the electron integral $F_m(\xi, k_\omega b)$ varies as k_ω^{-1}, provided the adiabaticity condition $\xi \ll 1$ is fulfilled. Dropping logarithmic factors, the probability varies as k_ω^{-1} or ω^{-1}. This behavior is seen in Fig. 1, where Eq. (22) is plotted for typical conditions. One sees both the surface plasmon at roughly $\omega_p/\sqrt{2}$ and the divergent $m=0$ excitation going to small ω.

IV. DIELECTRIC TUBES

There is much interest in carbon nanotubes composed of one or more graphite layers. We apply the dielectric theory by treating the structure as a dielectric tube with a finite wall thickness. Indeed this approximation has been used to model the electron response of C_{60} and carbon nanotubes.[15] Let us consider a dielectric tube with inner and outer radii R_1 and R_2. There will now be two surface layers producing the induced field, at the inner and outer surfaces. The derivation of the response proceeds as before to obtain a formula similar to Eq. (19). The tube response is conveniently expressed in terms of a 2×2 matrix $\mathbf{\Pi}_{mk}$ given by

$$\mathbf{\Pi}_{mk} = (1-\epsilon)\begin{pmatrix} -1+(\epsilon-1)x_1 K_m'(x_1) I_m(x_1) & (\epsilon-1)x_2 I_m'(x_1) K_m(x_2) \\ (e-1)x_1 K_m'(x_2) I_m(x_1) & 1+(\epsilon-1)x_2 I_m'(x_2) K_m(x_2) \end{pmatrix}^{-1},$$

where $x_{1,2} = kR_{1,2}$. Then the product $xI_m(x)I_m'(x)\,\mathrm{Im}\,\Pi_{mk}$ in Eq. (19) is replaced by

$$(x_1 I_m(x_1), x_2 I_m(x_2))\,\mathrm{Im}\,\mathbf{\Pi}_{mk}\begin{pmatrix} I_m'(x_1) \\ I_m'(x_2) \end{pmatrix}.$$

The poles of this function give the eigenmodes of the tube. This has been derived for the dielectric function of an ionic insulator in Ref. 12 and for an ideal conductor in Ref. 16. The conducting tube shows three strong peaks in EELS. These are shown in Fig. 2, calculated with a geometry of a typical carbon nanotube and the Drude dielectric function, Eq. (20). Instead of a single surface peak, the $m \neq 0$ modes split in two due to the interaction of the modes on the outer and inner surfaces. In Fig. 2, one sees these two modes as the peaks at 4.6 and 8.8 eV. In the limit of a thin-walled tube, the upper mode goes to the bulk plasmon frequency (10 eV in the calculation) and the lower mode goes to zero. Besides the two surface modes, there is a low-frequency $m=0$ mode that corresponds to charge conduction along the wire. As in the case of the solid conducting wire, the excitation probability goes to infinity as the frequency goes to zero.

It is not realistic to use a conductor dielectric function for carbon, and in Fig. 3 we show the graphite nanotube response using an empirical dielectric function of graphite. In principle, the dielectric function is anisotropic, which our derivation does not take into account. The empirical dielectric function[17] has a plateau in the imaginary part extending up to 5 eV, associated with π-electron transitions. This gives rise to the peak at 5 eV in Fig. 3. There is also a high-frequency component associated with σ electrons, peaking at 15 eV, which gives rise to the peak at slightly higher energy in Fig. 3. There is no indication of a low-frequency peak associated with conduction modes. Thus from the point of view of EELS, graphite behaves more like an insulator than a conductor. A similar spectrum was obtained from calculating the energy-loss rate for electrons going through carbon bundles.[18]

ACKNOWLEDGMENTS

We thank J. M. Chen, J. Rehr, and C. Colliex for discussions on this topic. G.F.B. was supported by the Department of Energy under Grant No. DE-FG-06-90ER-40561; H.E. was supported by the Department of Energy under Contract No. W-31-109-ENG-38; and B.R. was supported by DARPA Contract No. DABT63-95-C-0121.

[1] R. Kuzuo, M. Tarauchi, and M. Tanaka, Jpn. J. Appl. Phys., Part 2 **31**, L1484 (1992).
[2] B. W. Reed, J. M. Chen, N. MacDonald, and J. Silcox (private communication).
[3] K. Suenaga *et al.*, Science **278**, 653 (1997).
[4] Z. L. Wang, Micron **27**, 265 (1996).
[5] Y. T. Chu *et al.*, Part. Accel. **6**, 13 (1984).
[6] A. Rivacoba, P. Apell, and N. Zabala, Nucl. Instrum. Methods Phys. Res. B **96**, 465 (1995).
[7] L. Henrard and P. Lambin, J. Phys. B **29**, 5127 (1996).
[8] C. F. Bohren and D. R. Huffman, *Absorption and Scattering of Light by Small Particles* (Wiley, New York, 1983), Sect. 8.4.
[9] R. H. Ritchie, Phys. Rev. **106**, 874 (1957).
[10] J. D. Jackson, *Classical Electrodynamics* (Wiley, New York, 1962), Eq. 3.148.
[11] I. S. Gradshteyn and I. M. Ryzhik, *Table of Integrals, Series, and Products* (Academic, New York, 1980), Eq. 3.937.2.
[12] R. Englman and R. Ruppin, J. Phys. C **1**, 614 (1968).
[13] A. Gold and A. Ghazali, Phys. Rev. B **41**, 7626 (1980), Eq. (23a).
[14] Q. P. Li and S. Das Sarma, Phys. Rev. B **43**, 11 768 (1991), Eq. (2.13).
[15] D. Ostling *et al.*, J. Phys. B **29**, 5115 (1996).
[16] M. Lin and W.-K. Kenneth Shung, Phys. Rev. B **47**, 6617 (1993).
[17] E. A. Taft and H. R. Philipp, Phys. Rev. **138**, A197 (1965).
[18] M. F. Lin and D. S. Chuu, Phys. Rev. B **57**, 10 183 (1998).